

Supporting Material for “Stable climate simulations using a realistic GCM with neural network parameterizations for atmospheric moist physics and radiation processes”

List of Supplemental Materials:

Table S1. The hyperparameter search space. Note that the "Number of Hidden Layers" are used in the fully connected DNNs, "Residual blocks" are used in the ResDNNs, and each Residual block has two fully connected layers.

Figure S1. Spatial distribution of the precipitation STD across all 10 stable NN-Parameterizations for the prognostic simulation from 1999 to 2003.

Figure S2. Wave spectra of (a) a stable NN-Parameterization and (b) an unstable parameterization. The light blue background indicates where the phase speed is greater than 5 m/s and the growth rate is positive. The stability diagrams were obtained by coupling the linear responses of the NN-parametrizations with the simplified 2-D dynamics with a chosen base state, which is the normal convection background in the long-term prognostication in (a) and the initial state for the unreal gravity wave in Move S1 in (b).

Figure S3. Latitude-pressure cross-section of the zonal and annual mean (a) temperature and (b) specific humidity for NNCAM simulated from 2004 to 2008, with their differences from the SPCAM simulation from 1999 to 2003.

Figure S4. Global distribution of the temporal mean precipitation predicted using NNCAM from January 1, 2004, to December 31, 2008, for the (a) annual, (b) boreal summer (JJA), and (c) boreal winter (DJF).

Figure S5. Global distributions of the precipitation differences between (a & b) NNCAM and SPCAM and (c & d) CAM5 and SPCAM averaged over the boreal summer (left panels) and winter (right panels).

Figure S6. Similar to Figure. 7 but for the zonally averaged coefficient of determination (R^2) for (a) heating and (b) moistening predicted using the NN-Parameterization.

Movie S1. Mid-level (500 hPa) convective moistening rate in a realistic configured NNCAM in which we use the chosen unstable NN-Parameterization to parameterize convection. This movie records the first unrealistic wave in maritime continent.

Movie S2. Similar movie as Movie S1 but for two gravity wave afterwards in the same simulation.

Table S1. The hyperparameter search space. Note that the "Number of Hidden Layers" are used in the fully connected DNNs, "Residual blocks" are used in the ResDNNs, and each Residual block has two fully connected layers.

Hyperparameter Type	Hyperparameter Space
Number of Hidden Layers/Residual blocks	3, 4, 5, 6, 7, 8, 9
Width of Hidden Layers	64, 128, 256, 512, 1024
Learning rate	0.001, 0.002, 0.0001, 0.005
Dropout rate	0, 0.2, 0.3, 0.5
Batch size	128, 256, 512, 1024
Weight decay	0, 1e-5, 5e-4
Activation function	ReLU, Leaky-ReLU, Sigmoid
Loss function	Mean Squared Error
optimizers	Adam, SGD

Figure S1 – S6

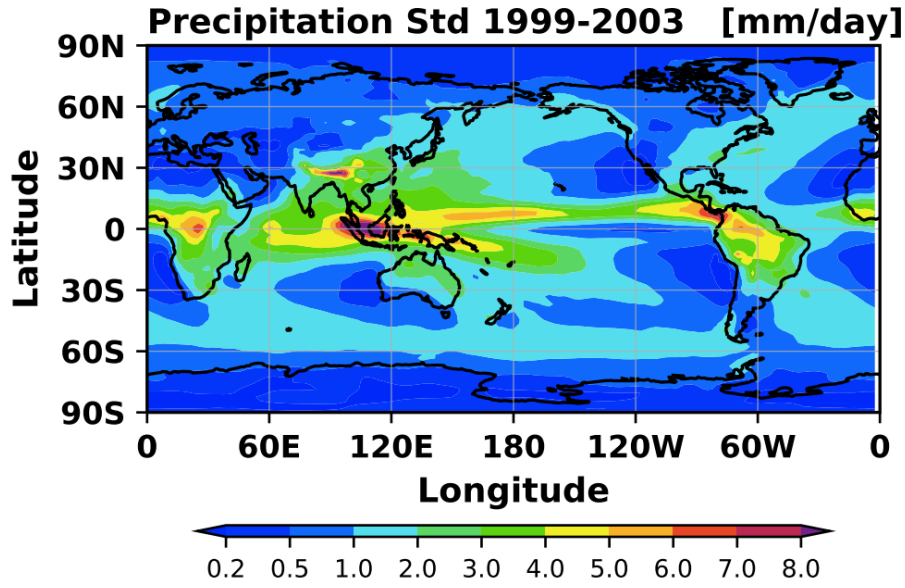


Figure S1. Spatial distribution of the precipitation STD across all 10 stable NN-Parameterizations for the prognostic simulation from 1999 to 2003.

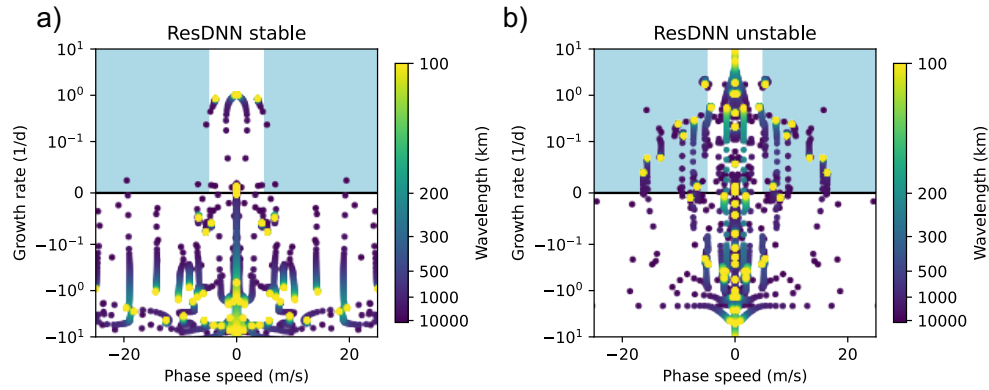


Figure S2. Wave spectra of (a) a stable NN-Parameterization and (b) an unstable parameterization. The light blue background indicates where the phase speed is greater than 5 m/s and the growth rate is positive. The stability diagrams were obtained by coupling the linear responses of the NN-parametrizations with the simplified 2-D dynamics with a chosen base state, which is the normal convection background in the long-term prognostication in (a) and the initial state for the unreal gravity wave in Move S1 in (b).

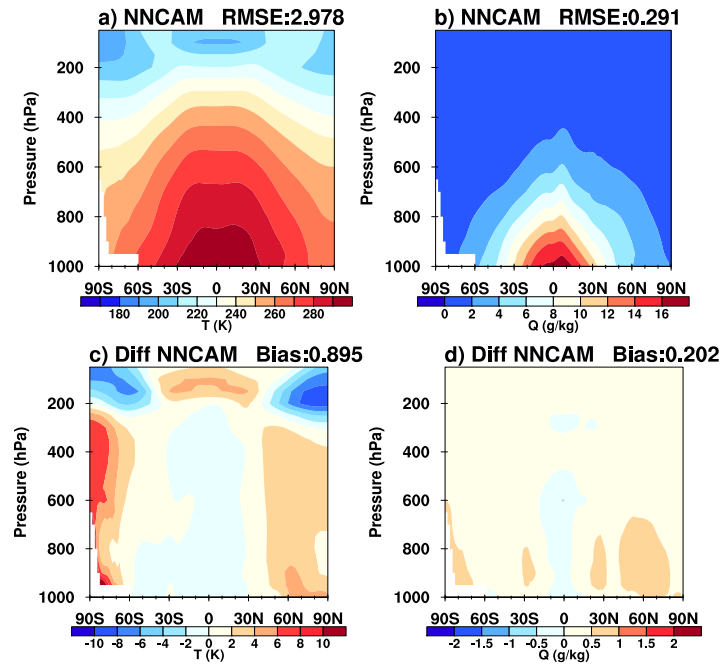


Figure S3. Latitude-pressure cross-section of the zonal and annual mean (a) temperature and (b) specific humidity for NNCAM simulated from 2004 to 2008, with their differences from the SPCAM simulation from 1999 to 2003.

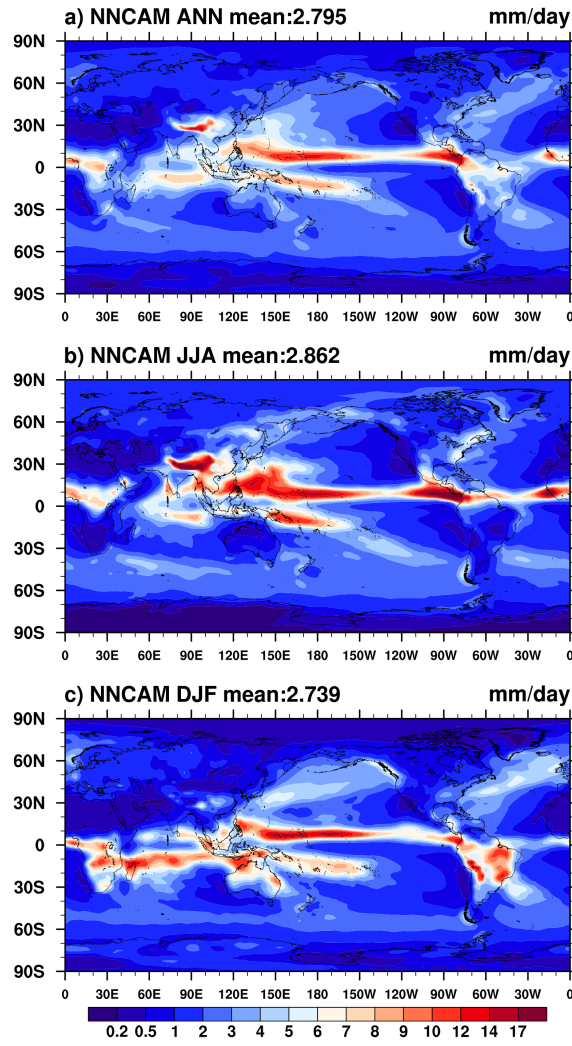


Figure S4. Global distribution of the temporal mean precipitation predicted using NNCAM from January 1, 2004, to December 31, 2008, for the (a) annual, (b) boreal summer (JJA), and (c) boreal winter (DJF).

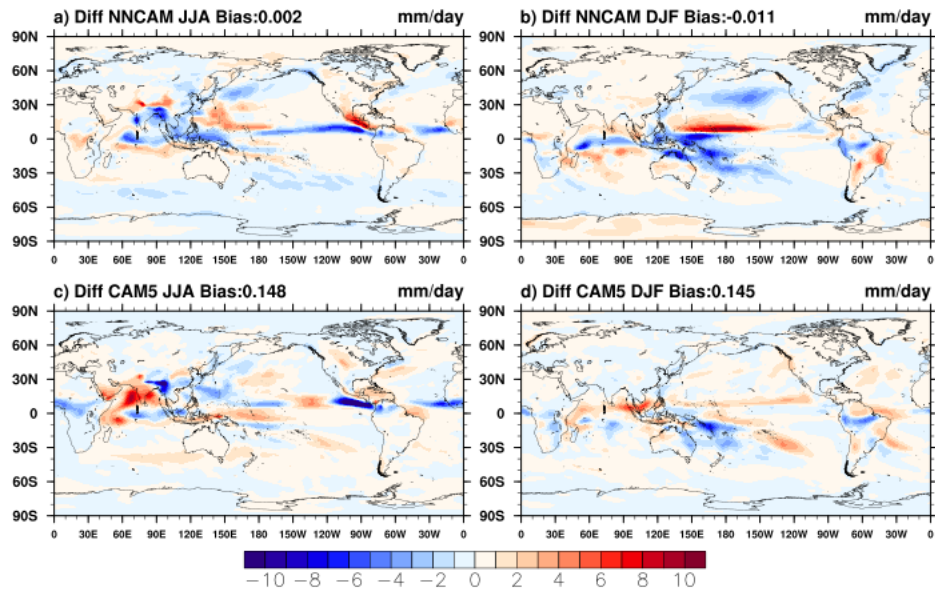


Figure S5. Global distributions of the precipitation differences between (a & b) NNCAM and SPCAM and (c & d) CAM5 and SPCAM averaged over the boreal summer (left panels) and winter (right panels).

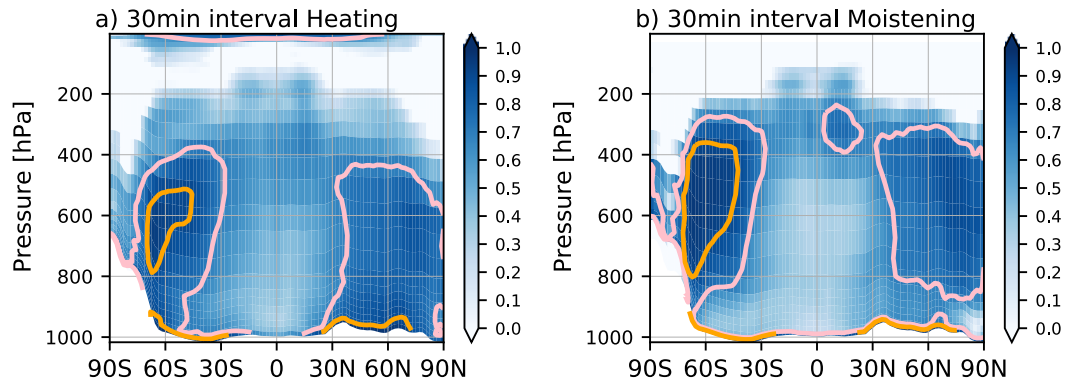


Figure S6. Similar to Figure. 7 but for the zonally averaged coefficient of determination (R^2) for (a) heating and (b) moistening predicted using the NN-Parameterization.